

Genome-wide Map of Nucleosome Acetylation and Methylation in Yeast

Dmitry K. Pokholok,^{1,4} Christopher T. Harbison,^{1,4} Stuart Levine,¹ Megan Cole,^{1,2} Nancy M. Hannett,¹ Tong Ihn Lee,¹ George W. Bell,¹ Kimberly Walker,¹ P. Alex Rolfe,³ Elizabeth Herbolzheimer,¹ Julia Zeitlinger,¹ Fran Lewitter,¹ David K. Gifford,^{1,3} and Richard A. Young^{1,2,*}

¹Whitehead Institute for Biomedical Research
Nine Cambridge Center
Cambridge, Massachusetts 02142

²Department of Biology
Massachusetts Institute of Technology
Cambridge, Massachusetts 02139

³MIT Computer Science and Artificial Intelligence
Laboratory
Cambridge, Massachusetts 02139

Summary

Eukaryotic genomes are packaged into nucleosomes whose position and chemical modification state can profoundly influence regulation of gene expression. We profiled nucleosome modifications across the yeast genome using chromatin immunoprecipitation coupled with DNA microarrays to produce high-resolution genome-wide maps of histone acetylation and methylation. These maps take into account changes in nucleosome occupancy at actively transcribed genes and, in doing so, revise previous assessments of the modifications associated with gene expression. Both acetylation and methylation of histones are associated with transcriptional activity, but the former occurs predominantly at the beginning of genes, whereas the latter can occur throughout transcribed regions. Most notably, specific methylation events are associated with the beginning, middle, and end of actively transcribed genes. These maps provide the foundation for further understanding the roles of chromatin in gene expression and genome maintenance.

Introduction

The genomes of eukaryotes are packaged into chromatin, the fundamental unit of which is the nucleosome. Nucleosomes consist of approximately 146 base pairs of DNA wrapped around a histone octamer (Luger et al., 1997). The histone components of nucleosomes and additional chromatin proteins can interact to form higher-order chromosomal structures. Nucleosomes are thus critical to the organization and maintenance of genetic material, and their position and modification state can profoundly influence genetic activities such as regulation of gene expression (Kouzarides, 2002; Narlikar et al., 2002).

Several recent studies have explored the relative occupancy and modification state of nucleosomes across the yeast genome by using chromatin immunoprecipitation

of histones and DNA-microarray analysis, a technique known as “genome-wide location analysis” or “ChIP-chip” (Bernstein et al., 2002, 2004; Kurdistani et al., 2004; Lee et al., 2004; Robyr et al., 2002; Santos-Rosa et al., 2002). The results of these studies, which used DNA microarrays that probed a single site in the intergenic or transcribed portions of the genome, suggested that the intergenic regions of *S. cerevisiae* are less densely occupied by nucleosomes than transcribed regions (Lee et al., 2004) and that nucleosome density in both regions inversely correlates with transcription rates (Bernstein et al., 2004; Lee et al., 2004). Similar studies have explored the relationship between transcription and genome occupancy by chromatin regulators (Humphrey et al., 2004; Kurdistani et al., 2002; Lieb et al., 2001; Ng et al., 2002b, 2003b; Robert et al., 2004; Robyr et al., 2002) or transcription and modification of nucleosomes (Kurdistani et al., 2004; Robyr et al., 2002; Roh et al., 2004). Some conclusions from these studies are difficult to reconcile with one another; for example, the histone acetyltransferases Gcn5 and Esa1 appear to be recruited to genes upon transcriptional activation (Robert et al., 2004), but acetylation of the amino acid residues they target in histones does not appear to be strongly associated with transcriptional activity (Kurdistani et al., 2004).

To more accurately define nucleosomal occupancy and modification and their relationships to transcription, we have investigated genome-wide chromatin structure at considerably higher resolution than that afforded by the experimental designs that have been used thus far. Such designs have typically used DNA microarrays with a single feature to capture signals from each intergenic or transcribed region (Bernstein et al., 2004; Kurdistani et al., 2004; Lee et al., 2004). We describe here profiling of protein-DNA occupancy at high resolution and accuracy using improved protocols and DNA microarrays that tile the yeast genome. The results we obtain with this approach provide a more complete picture of nucleosome occupancy and the nature of modifications associated with transcriptional activity, resolve discrepancies in previous reports, and allow us to produce the first high-resolution maps of histone acetylation and methylation in the yeast genome.

Results and Discussion

High-Resolution Genome-wide ChIP-Chip

To increase the resolution and accuracy of genome-wide location analysis, we designed a DNA microarray that contains over 40,000 probes for the yeast genome and developed hybridization methods that maximized signal-to-noise ratios on this array (see [Experimental Procedures](#)). To test whether these modifications improved the resolution and accuracy of genome-wide binding analysis, we explored the genome-wide occupancy of Gcn4, a transcriptional regulator of amino acid-biosynthetic genes with a well-characterized DNA

*Correspondence: young@wi.mit.edu

⁴These authors contributed equally to this work.

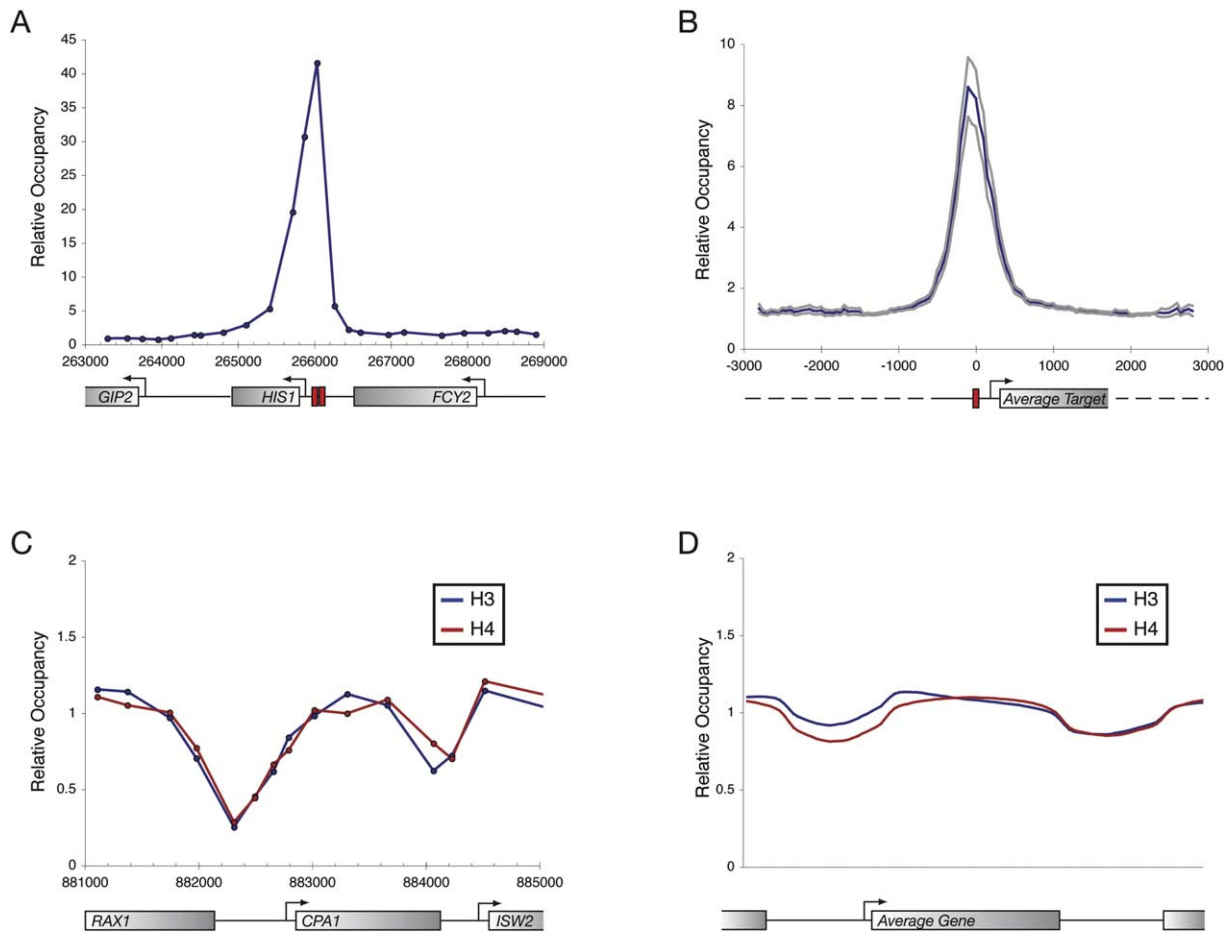


Figure 1. Nucleosome Occupancy across the Yeast Genome with High-Resolution Genome-wide Location Analysis

(A) Occupancy of the *HIS1* promoter by Gcn4. The genomic positions of probe regions are arrayed along the x axis, with the ratio of enrichment of Gcn4 for probes along the y axis. ORFs are depicted as gray rectangles, and arrows indicate the direction of transcription. Red boxes represent sequence matches to the Gcn4 binding specificity within promoter regions.

(B) Composite profile of Gcn4 binding at the set of 84 high-confidence Gcn4 target genes. Promoter and downstream regions were aligned with each other according to the position of a sequence match to the Gcn4 binding specificity. Aligned probes were then assigned to 50 bp segment bins, and an average of the corresponding enrichment ratio was calculated. Standard error of the mean is shown in gray. Genetic elements are depicted as in Figure 1A, except that dashed lines represent sites including both ORFs and intergenic regions.

(C) Nucleosome occupancy at the promoter of *CPA1*, a gene encoding an amino acid-biosynthetic enzyme. The genomic positions of probe regions are arrayed along the x axis, with the ratio of enrichment of histone H3 (blue) or H4 (red) for probes along the y axis. ORFs are depicted as gray rectangles, and arrows indicate the direction of transcription.

(D) A composite profile of histone occupancy at 5324 genes. The ends of ORFs were defined at fixed points according to the position of translational start and stop sites. The length of the ORF was then subdivided into 40 regions of equal length, and probes were assigned according to their nearest corresponding relative position. Probes in promoter regions were similarly assigned following subdivision into 20 regions. The average histone H3 (blue) or H4 (red) enrichment for each subdivided bin is plotted.

binding specificity (Hope and Struhl, 1985; Oliphant et al., 1989), crystal structure (Ellenberger et al., 1992; O'Shea et al., 1991), and previously identified target genes (Arndt and Fink, 1986; Natarajan et al., 2001). The binding data for individual target genes are shown in Figure 1A and in Figure S1 in the Supplemental Data available with this article online. For those regions for which there is strong evidence for Gcn4 binding, we found that the peak of Gcn4 binding occurred directly over that binding site.

To test the accuracy of the new method, we identified a test set of 84 genes most likely to be targeted by Gcn4 in vivo (Figure 1B, Table S1, Experimental Pro-

cedures) and a set of 945 genes least likely to be targeted by Gcn4; the selection criteria for these sets of genes is described in Experimental Procedures. Based on these positive and negative Gcn4 targets, analysis of Gcn4 binding with the new method suggests a false-positive rate of less than 1% and a false-negative rate of ~25%, corresponding with a total of 210 genes whose promoters are bound within the optimal p value threshold of 6×10^{-6} (Experimental Procedures). These results demonstrate that the new array and protocol modifications provide substantially higher resolution and accuracy than our previous method using self-printed arrays (Harbison et al., 2004; Lee et al., 2002).

Global Nucleosome Occupancy

The improved accuracy and resolution of this ChIP-Chip method was used to investigate nucleosome occupancy and modification throughout the yeast genome. When we examined histone occupancy with antibodies against core histone H3 or histone H4, using genomic DNA as the reference channel, we found a relatively high density of nucleosomes over transcribed regions and a lower density over intergenic regions (Figures 1C and 1D). Figure 1C shows a stereotypical example of histone occupancy at a portion of chromosome XV. Figure 1D presents composite profiles of histone H3 and H4 for 5324 genes aligned according to the location of translation initiation and termination sites. There was an ~20% reduction in histone occupancy in intergenic sequences relative to genic sequences for the average gene. These results are consistent with previous observations (Lee et al., 2004) and suggest that the majority of yeast genes have higher nucleosome density over transcribed regions relative to intergenic regions.

We were surprised to find that differential enrichment of intergenic and genic regions also occurred in control experiments lacking antibody (compare Figure 2A and Figure 1D). Results similar to those in Figure 2A were obtained in control experiments when ChIPs were performed with antibodies directed against nonhistone proteins (data not shown). Others have noted that different relative levels of intergenic and genic DNA are recovered using various extraction strategies (Nagy et al., 2003), but control data of this type have not yet been used to normalize the results of histone ChIP studies (Bernstein et al., 2004, 2005; Kurdistani et al., 2004; Lee et al., 2004). When these control experiments were used to normalize the histone H3 data, we found that there were not substantial differences in the relative levels of intergenic versus genic DNA at the average gene (Figure 2B). Nonetheless, approximately 40% of yeast promoters do have lower levels of histones than their downstream transcribed regions, even after the normalization by control experiments (Figure S2), and we show below that these are associated with transcribed genes.

To examine the relationship between gene expression and nucleosome occupancy, we assigned genes into five different classes depending on their transcriptional rate (Holstege et al., 1998) and created a composite histone H3 profile for each class (Figures 2C and 2D). The composite histone profile in Figure 2C was generated by using whole genomic DNA in the reference channel, and that in Figure 2D was generated by normalizing to a no-antibody control ChIP. The results in both profiles confirm that nucleosome occupancy at both promoter and transcribed regions inversely correlates with gene activity, in agreement with previous gene-specific and genome-wide studies (Bernstein et al., 2004; Boeger et al., 2003; Lee et al., 2004; Reinke and Horz, 2003). The results shown in Figure 2D also suggest that nucleosome occupancy is reduced maximally at the promoters of active genes. In contrast, the promoters of transcriptionally inactive genes are as densely populated with nucleosomes as genic regions.

If gene activation leads to reduced nucleosome occupancy, then dynamic activation of specific genes should cause reduced histone levels at these newly

transcribed genes. To test this notion, we performed ChIP-Chip with histone antibodies on cells before and after exposure to oxidative stress (Causton et al., 2001). At genes known to be activated by oxidative stress (e.g., *HSP30* and *HSP82*), nucleosome occupancy dropped substantially (Figure S3). These results confirm that gene activation leads to reduced nucleosome density in both promoter and transcribed regions, with the greatest effect occurring at the promoter.

Histone Acetylation

The histone acetylases Gcn5 and Esa1 are generally recruited to the promoter regions of active genes (Robert et al., 2004), and thus we would expect that the amino acid residues that are substrates of these HATs would be preferentially acetylated at active genes. A recent genome-wide study, however, reported little correlation between transcriptional activity and acetylation of the histone H3 and H4 amino acid residues targeted by Gcn5 and Esa1 (Kurdistani et al., 2004). To understand the source of these discrepancies, we used the new methods to investigate selected histone modifications genome-wide.

Histone H3 lysine 9 acetylation (H3K9ac) and histone H3 lysine 14 acetylation (H3K14ac) are among the modifications catalyzed by Gcn5 (Kuo et al., 1996; Utley et al., 1998; Zhang et al., 1998). We used ChIP-Chip to measure the levels of H3K9ac relative to the levels of core histone H3 genome-wide. The results show that acetylation of histone H3 at lysine 9 peaks at the predicted transcriptional start sites of active genes (Figure 3A) and that this modification correlates with transcription rates genome-wide (Figure 3B). We also found that acetylation of histone H3 at lysine 14 peaks over the start sites of active genes (Figure 3C) and correlates with transcription rates genome-wide (Figure 3D). We conclude that there is a positive association between Gcn5, the modifications known to be catalyzed by Gcn5, and transcriptional activity (Figure 3 and Figure S4A).

Four lysine residues of histone H4 are acetylated by Esa1, an acetyltransferase associated with the NuA4 complex (Allard et al., 1999; Clarke et al., 1999; Vogelauer et al., 2000). We measured the levels of hyperacetylated histone H4 relative to core histone genome-wide using ChIP-Chip with an antibody that recognizes histone H4 acetylated at lysines 5, 8, 12, and 16 (H4K5ac8ac12ac16ac). The results showed that H4 hyperacetylation peaks over the start sites of active genes (Figure 3E) and correlates with transcription rates (Figure 3F), although the association is not as strong as that observed for H3K9ac and H3K14ac. Our analysis cannot exclude the possibility that acetylation of individual lysine residues in the N-terminal tail of histone H4 might correlate differently with transcriptional activity. Nonetheless, our data reveal a positive, albeit modest, correlation between Esa1 occupancy, the modifications known to be catalyzed by this enzyme, and transcriptional activity (Figure 3 and Figure S4B).

To ascertain whether dynamic gene activation leads to the expected increase in histone acetylation at sites catalyzed by Gcn5 and Esa1, we performed ChIP-Chip with the relevant histone antibody on cells before and

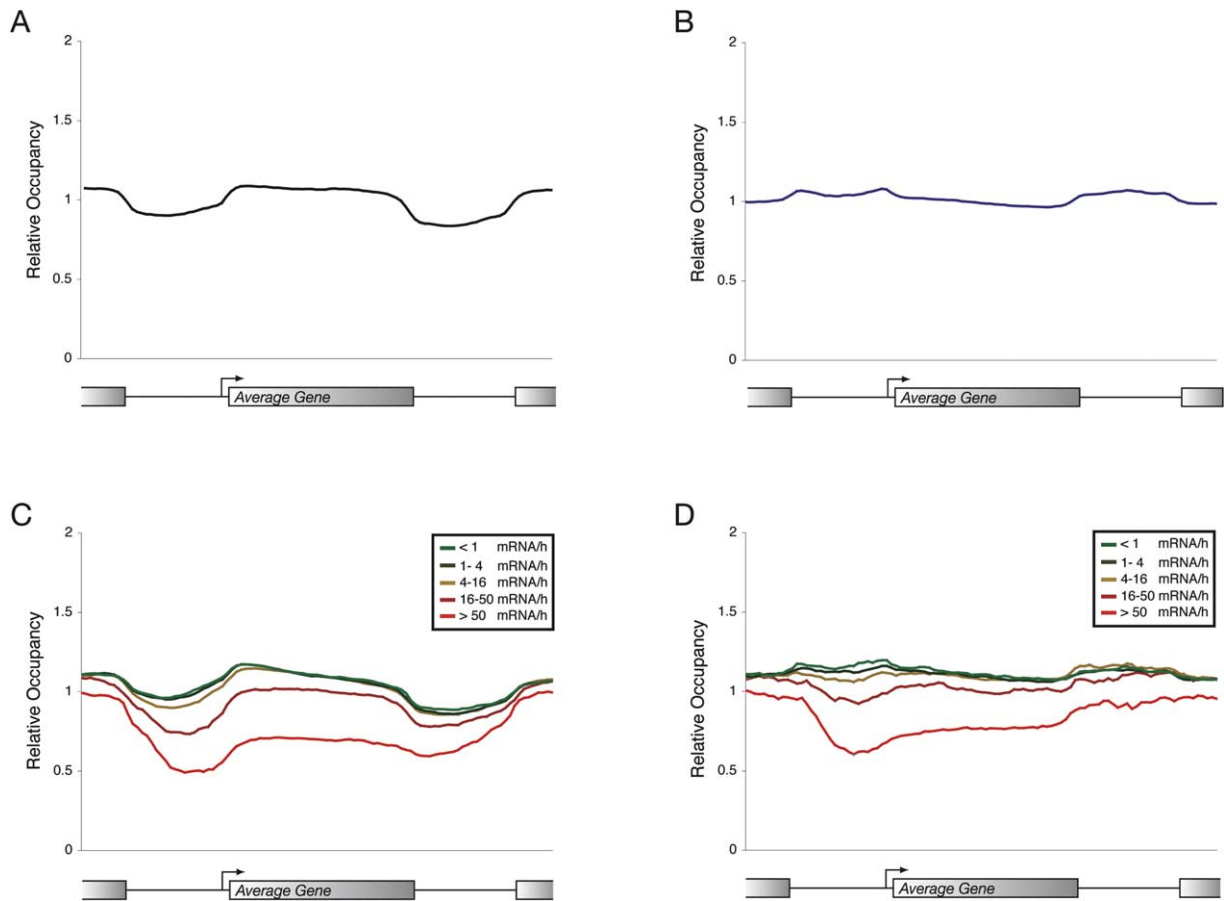


Figure 2. Comparisons of Histone Profiles

- (A) A composite profile of enrichment in a control experiment. The profile is created as in Figure 1D, except that enrichment is measured from a mock immunoprecipitation, in which no antibody has been included (Experimental Procedures).
- (B) A composite profile of histone occupancy normalized to a control. The profile is created as in Figure 1D, except that enrichment from H3 immunoprecipitation is normalized to enrichment from mock immunoprecipitations.
- (C) A composite profile of histone occupancy according to transcriptional activity. All genes for which data were available (Holstege et al., 1998) were divided into five classes according to their transcriptional rate. Composite data were computed for H3 enrichment as in Figure 1D.
- (D) A composite profile of normalized histone occupancy according to transcriptional activity. The composite profile is created as in Figure 2C, except that enrichment from H3 immunoprecipitation is normalized to enrichment from mock immunoprecipitations.

after exposure to oxidative stress. The results confirm that gene activation leads to increased histone acetylation at sites catalyzed by Gcn5 and Esa1 in the promoter and transcribed regions of activated genes (Figure S5).

In general, we find that histones with the acetylated residues studied here are enriched predominantly at promoter regions and transcriptional start sites of active genes and that enrichment drops substantially across the ORFs (Figure 3 and Figure S5). This is consistent with the model that transcriptional activators generally recruit Gcn5 and Esa1 to promoters of genes upon their activation (Robert et al., 2004) and with the idea that the two HATs acetylate local nucleosomes when recruited to these genes. Our conclusion that there is a strong correlation between transcriptional activity and acetylation of the histone H3 and H4 amino acid residues targeted by Gcn5 and Esa1 is in contrast to that of Kurdistani et al. (2004). This discrepancy is most likely due

to differences in the material used in the control channel in the ChIP-Chip procedure. The experiments described here compare ChIP with a histone-modification antibody to a control ChIP with a core histone antibody. The experiments reported in Kurdistani et al. (2004) used whole genomic DNA in the reference channel. We found we could replicate the results in Kurdistani et al. (2004) if we used whole genomic DNA as a reference in ChIP-Chip experiments (Figure S6), but for reasons described above, this method of normalization is inappropriate.

Histone Methylation

Methylation of histones in *S. cerevisiae* is carried out by three known histone methyltransferases, which are capable of covalently modifying specific lysine residues in histone H3 with up to three methyl groups (Peterson and Laniel, 2004). Since characterization of specific methylation marks has been studied primarily at the

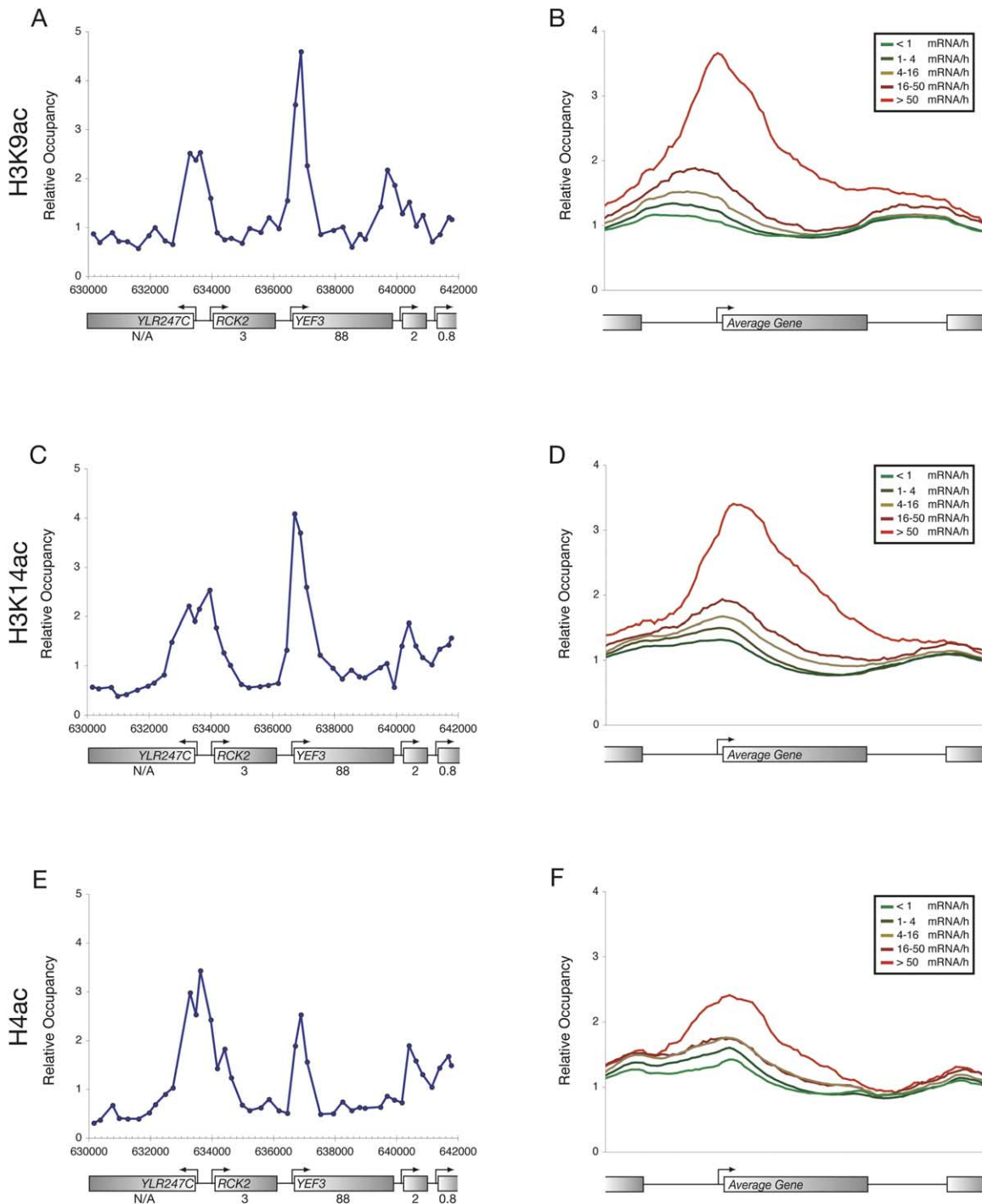


Figure 3. Nucleosome Acetylation Generally Correlates with Transcriptional Activity

(A) Acetylation of H3K9 at a locus on chromosome XII. Enrichment is depicted as in Figure 1. The number beneath each gene represents the transcriptional frequency of the corresponding ORF (Holstege et al., 1998) in mRNA/hr.

(B) Composite profile of acetylation of H3K9 across the average gene. Composite profiles of acetylation according to transcriptional-frequency class are shown as in Figure 2.

(C) Acetylation of H3K14 at a locus on chromosome XII. Enrichment is depicted as in Figure 1. The number beneath each gene represents the transcriptional frequency of the corresponding ORF (Holstege et al., 1998) in mRNA/hr.

(D) Composite profile of acetylation of H3K14 across the average gene. Composite profiles of acetylation according to transcriptional-frequency class are shown as in Figure 2.

(E) Hyperacetylation of H4 at a locus on chromosome XII. Enrichment is depicted as in Figure 1. The number beneath each gene represents the transcriptional frequency of the corresponding ORF (Holstege et al., 1998) in mRNA/hr.

(F) Composite profile of hyperacetylation of H4 across the average gene. Composite profiles of acetylation according to transcriptional-frequency class are shown as in Figure 2.

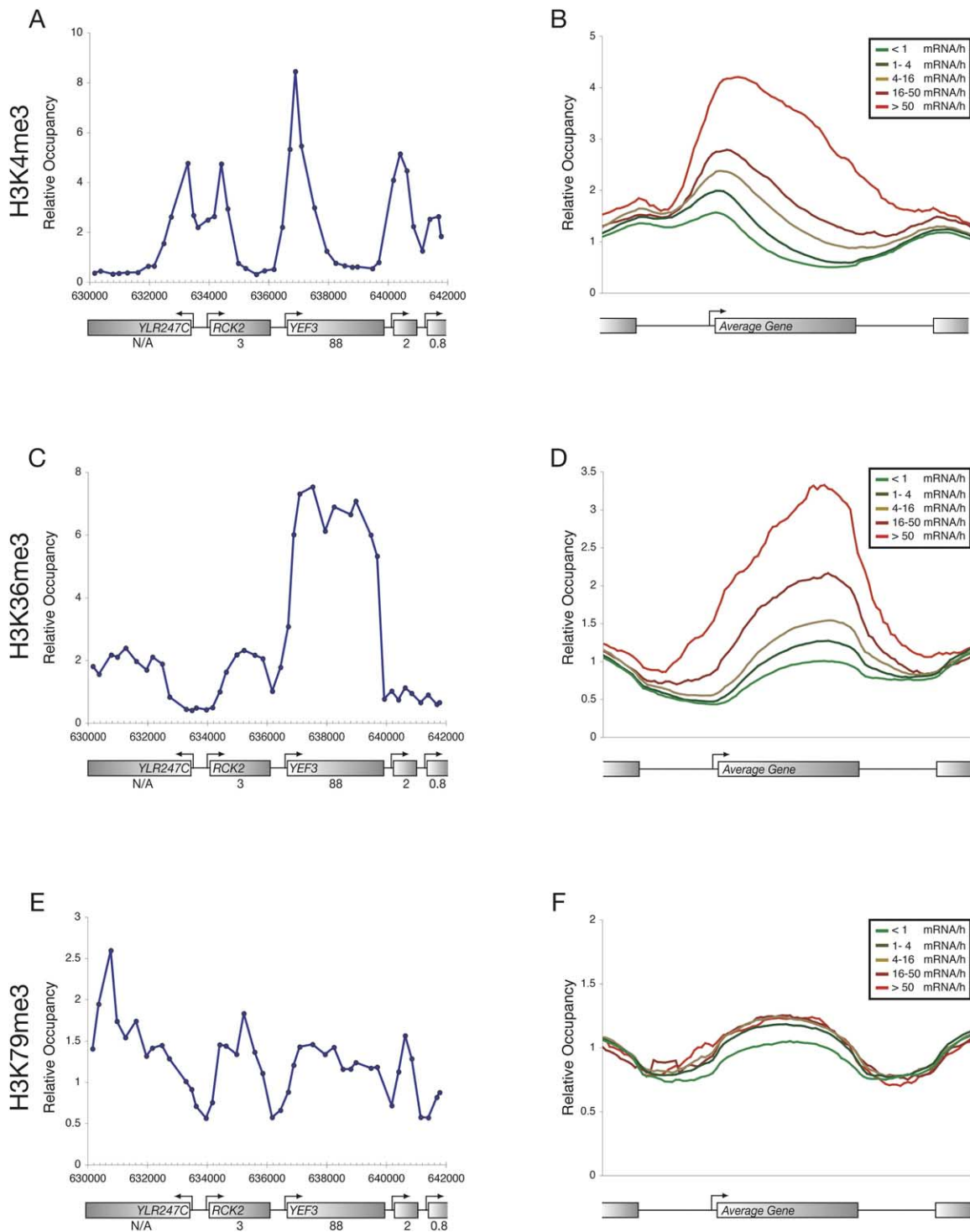


Figure 4. Nucleosome Methylation Generally Correlates with Transcriptional Activity

(A) Trimethylation of H3K4 at a locus on chromosome XII. Enrichment is depicted as in Figure 1. The number beneath each gene represents the transcriptional frequency of the corresponding ORF (Holstege et al., 1998) in mRNA/hr.

(B) Composite profile of trimethylation of H3K4 across the average gene. Composite profiles of methylation according to transcriptional-frequency class are shown as in Figure 2.

(C) Trimethylation of H3K36 at a locus on chromosome XII. Enrichment is depicted as in Figure 1. The number beneath each gene represents the transcriptional frequency of the corresponding ORF (Holstege et al., 1998) in mRNA/hr.

(D) Composite profile of trimethylation of H3K36 across the average gene. Composite profiles of methylation according to transcriptional-frequency class are shown as in Figure 2.

(E) Trimethylation of H3K79 at a locus on chromosome XII. Enrichment is depicted as in Figure 1. The number beneath each gene represents the transcriptional frequency of the corresponding ORF (Holstege et al., 1998) in mRNA/hr.

(F) Composite profile of trimethylation of H3K79 across the average gene. Composite profiles of methylation according to transcriptional-frequency class are shown as in Figure 2.

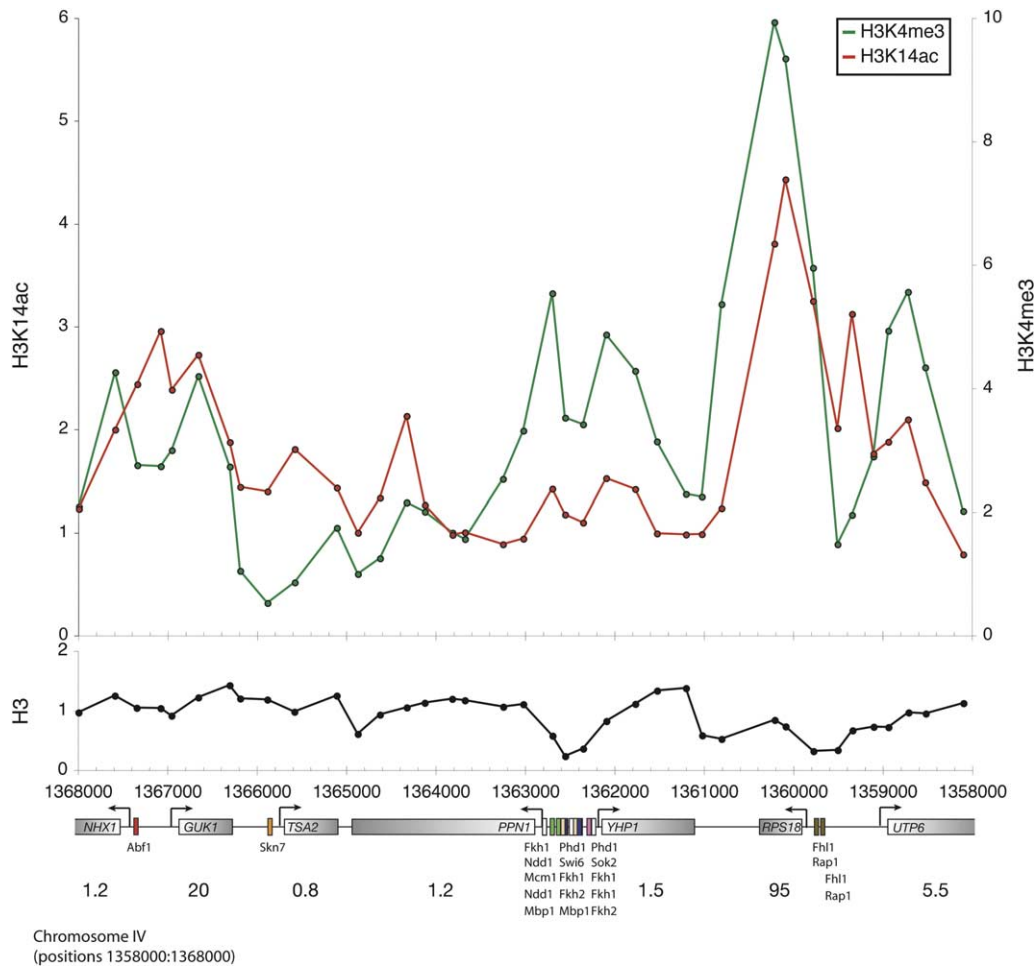


Figure 5. A High-Resolution Genome-wide Map of Nucleosome States

A map for a region on chromosome IV is depicted as in Figure 1. Conserved binding sites for transcriptional regulators (Harbison et al., 2004) are depicted as colored boxes. Numbers beneath genes represent transcriptional activity (mRNA/hr). Enrichment values from acetylated H3K14, trimethylated H3K4, and histone H3 are depicted in red, green, and black, respectively.

level of individual genes (Bannister et al., 2005; Bernstein et al., 2002; Krogan et al., 2003b; Ng et al., 2003a; Xiao et al., 2003), we sought to systematically profile mono-, di-, and trimethylated residues at K4, K36, and K79 of histone H3 in nucleosomes associated with genomic DNA.

The histone methyltransferase Set1 has previously been shown to be recruited to the 5' end of actively transcribed genes where it is responsible for histone H3K4 methylation (Bernstein et al., 2002; Briggs et al., 2001; Krogan et al., 2003a; Ng et al., 2003b; Santos-Rosa et al., 2002). We measured histone H3K4 trimethylation (H3K4me3) using ChIP-Chip and found that the results confirm previous studies (Santos-Rosa et al., 2002) and provide a higher-resolution picture of H3K4 trimethylation across the yeast genome (Figures 4A and 4B). Peaks of histone H3K4 trimethylation occurred at the beginning of actively transcribed genes, and there was a positive correlation between this modification and transcription rates (Figures 4A and 4B).

We also investigated the profiles of mono- and di-

methylated histone H3K4-containing nucleosomes and found that they exhibit a pattern distinct from that observed for trimethylated histone H3K4 (Figure S7). While trimethylated H3K4 peaks at the beginning of the transcribed portions of genes, dimethylated H3K4 (H3K4me2) is most enriched in the middle of genes, and monomethylated H3K4 (H3K4me) is found predominantly at the end of genes.

We measured genome-wide the relative levels of H3K36 trimethylation, which is catalyzed by Set2, a factor associated with the later stages of transcriptional elongation (Strahl et al., 2002). In contrast to the pattern observed with H3K4 trimethylated histones, we found that trimethylated H3K36 (H3K36me3) was enriched throughout the coding region, peaking near the 3' ends of transcription units (Figures 4C and 4D). H3K36 trimethylation also correlated with transcriptional activity. These results are consistent with the model that Set2 is recruited by the transcription elongation apparatus and that it methylates local nucleosomes during active transcription.

Table 1. Antibodies Used in This Study

Specificity	Supplier	Catalog #
Anti-Histone H3	Abcam	ab1791
Anti-Histone H4	Abcam	ab10156
Anti-H3K9ac	Upstate Biotechnology	06-942
Anti-H3K14ac	Upstate Biotechnology	06-911
Anti-H4ac	Upstate Biotechnology	06-866
Anti-H3K4me3	Abcam	ab8580
Anti-H3K4me2	Abcam	ab7766
Anti-H3K4me1	Abcam	ab8895
Anti-H3K36me3	Abcam	ab9050
Anti-H3K79me3	Abcam	ab2621
Anti-myc	Taconic Biotechnology	9E11
Rabbit IgG	Upstate Biotechnology	12-370

The Dot1 histone methyltransferase modifies histone H3 lysine 79 (H3K79), which occurs within the core domain of histone H3 (Feng et al., 2002; Ng et al., 2002a, 2003a). Methylation of this residue is estimated to occur in ~90% of all histones and is associated with telomeric silencing control in yeast (Ng et al., 2003a; van Leeuwen et al., 2002), but global ChIP profiles of dimethylated H3K79 in *Drosophila* (Schubeler et al., 2004) have linked this modification to active transcription. We investigated the genomic profile of H3K79 trimethylation in yeast (H3K79me3) and found that histones with this modification are enriched within the transcribed regions of genes (Figures 4E and 4F). Most genes appeared to have nucleosomes modified at H3K79; there was little correlation between the relative levels of H3K79 trimethylation at genes and transcriptional activity (Figure 4F).

Global Map of Histone Marks

We recently mapped the locations of conserved transcription-factor binding sites throughout the yeast genome (Harbison et al., 2004). We used the results described here to generate a complementary genome-wide map of nucleosome occupancy and histone modifications that includes results for eight sets of histone modifications (H3K9ac, H3K14ac, H4K5ac8ac12ac16ac, H3K4me1, H3K4me2, H3K4me3, H3K36me3, and H3K79me3). A portion of this map is shown in Figure 5, and a browsable form of the complete yeast-genome chromatin map is available at the authors' website (<http://web.wi.mit.edu/young/nucleosome>).

Concluding Remarks

It is well established that nucleosomes play fundamentally important roles in the organization and maintenance of the genome. Nucleosome modifications have been shown to be associated with transcriptional regulation at well-studied genes, and models have emerged that connect regulation of gene expression to histone modification by specific chromatin regulators (Cosma et al., 1999; Gregory et al., 1999; Kuo et al., 1998; Reinke and Horz, 2003). We have carried out a systematic genome-wide analysis of nucleosome acetylation and methylation at sufficient resolution to determine whether models that connect regulation of gene expression to histone modification (Deckert and Struhl, 2001; Reid et

al., 2000; Reinke et al., 2001; Suka et al., 2002) apply to gene regulation throughout the yeast genome.

The results described here, taken together with recent discoveries, are consistent with the following general model connecting gene expression to histone modification. Transcriptional activation by DNA binding regulators generally involves recruitment of Gcn5 and Esa1 to promoters, where these HATs acetylate specific residues on histones H3 and H4 at local nucleosomes (Figure 3) (Bhaumik and Green, 2001; Cosma et al., 1999; Larschan and Winston, 2001; Reid et al., 2000). We were able to find few exceptions to this general rule, where only one or the other HAT acetylates its target residues at the promoters of actively transcribed genes (data not shown). Active transcription is characteristically accompanied by histone H3K4 trimethylation by Set1 at the beginning of genes (Figure 4B) and by H3K4 dimethylation and monomethylation at nucleosomes positioned further downstream in the transcription unit (Figure S7) (Krogan et al., 2003a; Ng et al., 2003b). As the transcription apparatus proceeds down the transcription unit, increasing levels of histone H3K36 trimethylation are observed at most active genes, catalyzed by Set2 (Figure 4D) (Krogan et al., 2003b; Strahl et al., 2002). Histone H3K79me3, which is catalyzed by Dot1 (Feng et al., 2002; Ng et al., 2003a; van Leeuwen et al., 2002), is enriched within genes, but, unlike the other modifications studied here, this enrichment is not clearly associated with active transcription (Figure 4F). Correlations between transcriptional activity and histone occupancy or modification at intergenic and transcribed regions are summarized in Table S2.

The genome-wide maps of histone occupancy and modification described here should provide investigators with information useful for further exploring the histone code and its implications for gene regulation and chromosome organization and maintenance. We expect that the approaches used here to map histone occupancy and modification in yeast can also be used to gain insights into the linkage between gene expression and histone modification across the genome in higher eukaryotes.

Experimental Procedures

A detailed protocol of the ChIP-chip procedure, the microarray data described herein, and a description of the error model used for data analysis are available at the authors' website (<http://web.wi.mit.edu/young/nucleosome>).

Array Design

The Agilent DNA microarray used here has 44,290 features consisting of 60-mer oligonucleotide probes. The array covers 12 Mb of the yeast genome (85%), excluding highly repetitive regions, with an average probe density of 266 bp. Intergenic regions are represented by 14,256 probes, and ORFs are represented by 27,185 probes. The remaining 2,849 features included blank spots and controls.

Epitope Tagging, Antibodies, and Strains

Transcriptional and chromatin regulators were tagged at the C terminus with a 9-copy myc epitope. The sequence encoding the myc epitope was introduced into the endogenous gene immediately upstream of the stop codon. Specific oligonucleotides were used to generate PCR products from plasmids described by Cosma et al. (1999). The resulting PCR products were transformed into a W303

yeast to generate the tagged strains by one-step genomic integration. Clones were selected for growth on the appropriate selective media plates, and the insertion was confirmed by PCR. The expression of the epitope-tagged protein was confirmed by Western blotting using an anti-Myc (9E11). The antibodies used in this study are listed in Table 1.

Chromatin Immunoprecipitation and Genome-wide ChIP-Chip

Chromatin immunoprecipitation and genome-wide location analysis were performed as described previously (Ren et al., 2000), except that the crosslinking time was reduced to 30 min at room temperature, the order of Proteinase K and RNase treatment was reversed, and high-resolution oligonucleotide arrays (Agilent Technologies) were used for hybridizations. Briefly, yeast cells were grown in at least two independent cultures in rich medium. Response to hydrogen peroxide was induced by adding hydrogen peroxide to the cell cultures grown at mid-log phase in YPD medium at 30°C to final concentration of 0.4 mM for 20 min. Cultures were treated with formaldehyde (1%) for 30 min, and cells were collected by centrifugation, washed with ice-cold TBS, and disrupted by vortexing in lysis buffer in the presence of glass beads. The chromatin was sonicated to yield an average DNA fragment of 500 bp. The DNA fragments crosslinked to the proteins were enriched by immunoprecipitation with specific antibodies. After reversal of the crosslinks and purification, the immunoprecipitated and input DNA was labeled by ligation-mediated PCR with Cy5 and Cy3 fluorescent dyes, respectively. Both pools of labeled DNA were hybridized to a single DNA microarray (described above). Images of Cy5 and Cy3 fluorescence intensities were generated by scanning array using GenePix 5000 scanner and were analyzed with GenePix Pro 5.1 software. Experiments were carried out at least in duplicate.

We and other groups have noted that there can be modest differences in the relative levels of intergenic and genic yeast DNA that are recovered during phenol extraction (Nagy et al., 2003). Experimental analysis indicates that this is not due to differences in our ability to detect intergenic and genic DNA on the DNA microarrays. Our experiments also indicate that this observation is not due to artifacts due to differential labeling of DNA. Others have speculated that differential recovery is due to contaminating nucleases that might preferentially digest intergenic DNA (Nagy et al., 2003). It is also possible that there are intrinsic differences in susceptibility to shearing by sonication in intergenic and genic DNA.

Mock-Immunoprecipitation Normalization

Control immunoprecipitations were performed as above with two exceptions. In one case, an antibody with no specificity to histones (rabbit IgG) was substituted for the H3- or H4-specific antibody. In the second case, no antibody was added during the overnight incubation with magnetic beads. For histone H3 and H4 (data not shown), data were normalized relative to the “no antibody” control. Distributions of relative occupancy at ORF and intergenic regions by histone H3 are depicted in Figure S8. Following normalization by this method, the standard deviation is 0.38, and we used two-sampled t tests to determine the likelihood of differences occurring by chance in both the original and controlled experiments (Figure S8).

Data Analysis

Genome-wide location data were subjected to quality-control filters and median normalized, and the weighted average ratio of immunoprecipitated to control DNA was determined for each spot across all replicates. A confidence value (p value) for single probes and an averaged confidence value for neighboring probes were calculated.

A binding cutoff for Gcn4 was determined by comparing maximum IP/WCE ratios to a high-likelihood positive list and a high-likelihood negative list using ROC curve analysis. A positive list of 84 genes (Table S1) was selected on the basis of previous high-confidence binding data ($p \leq 0.001$) (Harbison et al., 2004), the presence of a perfect or near perfect Gcn4 consensus binding site (TGASTCA) in the region of -400 bp to +50 bp, and a greater than 2-fold change in steady-state mRNA levels dependent on Gcn4

when shifted to amino acid starvation medium (Natarajan et al., 2001). The negative list of 945 genes not transcribed from divergent intergenic regions was selected by weak binding ($p \geq 0.1$), absence of a motif near the presumed start site, and a less than 60% change in steady-state mRNA levels in response to shift to amino acid starvation. Each gene was scored based on the minimum p value found in the region -250 bp to +50 bp from the UAS using the higher of the single and averaged confidence score. Optimal parameters were determined by maximizing the absolute difference in identified genes in both the positive list and the negative list using the Statistics-ROC package for Perl.

Nucleosome-depleted promoters were defined as intergenic regions upstream of protein-coding genes for which unmodified histone H3 or H4 enrichment met the following criterion: the enrichment of any probe within the intergenic region was less than the average ratio of enrichment at two neighboring ORFs.

Throughout the text, histone H3 occupancy is often referred to as nucleosome occupancy. There are two reasons to believe that the results with H3 likely reflect nucleosome occupancy and not nucleosomes that are missing H3 specifically. First, we obtained similar results in independent experiments with H3 and H4. Second, previous in vitro studies suggest that it is H2A-H2B dimers (and not H3 or H4) that preferentially dissociate from nucleosomes during transcription (Kireeva et al., 2002).

Supplemental Data

Supplemental Data include two tables and eight figures and can be found with this article online at <http://www.cell.com/cgi/content/full/122/4/517/DC1/>.

Acknowledgments

We thank E. Fraenkel for helpful discussions and D. Reynolds for technical assistance. This work was supported by NHGRI grant HG002668 and NIH grant GM069676. T.I.L., D.K.G., and R.A.Y. consult for Agilent Technologies.

Received: April 25, 2005

Revised: June 1, 2005

Accepted: June 8, 2005

Published: August 25, 2005

References

- Allard, S., Utley, R.T., Savard, J., Clarke, A., Grant, P., Brandl, C.J., Pillus, L., Workman, J.L., and Cote, J. (1999). NuA4, an essential transcription adaptor/histone H4 acetyltransferase complex containing Esa1p and the ATM-related cofactor Tra1p. *EMBO J.* 18, 5108–5119.
- Arndt, K., and Fink, G.R. (1986). GCN4 protein, a positive transcription factor in yeast, binds general control promoters at all 5' TGACTC 3' sequences. *Proc. Natl. Acad. Sci. USA* 83, 8516–8520.
- Bannister, A.J., Schneider, R., Myers, F.A., Thorne, A.W., Crane-Robinson, C., and Kouzarides, T. (2005). Spatial distribution of di- and tri-methyl lysine 36 of histone H3 at active genes. *J. Biol. Chem.* 280, 17732–17736.
- Bernstein, B.E., Humphrey, E.L., Erlich, R.L., Schneider, R., Bouman, P., Liu, J.S., Kouzarides, T., and Schreiber, S.L. (2002). Methylation of histone H3 Lys 4 in coding regions of active genes. *Proc. Natl. Acad. Sci. USA* 99, 8695–8700.
- Bernstein, B.E., Liu, C.L., Humphrey, E.L., Perlestein, E.O., and Schreiber, S.L. (2004). Global nucleosome occupancy in yeast. *Genome Biol.* 5, R62. Published online August 20, 2004.. 10.1186/gb-2004-5-9-r62
- Bernstein, B.E., Kamal, M., Lindblad-Toh, K., Bekiranov, S., Bailey, D.K., Huebert, D.J., McMahon, S., Karlsson, E.K., Kulbokas, E.J., 3rd, Gingeras, T.R., et al. (2005). Genomic maps and comparative analysis of histone modifications in human and mouse. *Cell* 120, 169–181.
- Bhaumik, S.R., and Green, M.R. (2001). SAGA is an essential in vivo

- target of the yeast acidic activator Gal4p. *Genes Dev.* **15**, 1935–1945.
- Boeger, H., Griesenbeck, J., Strattan, J.S., and Kornberg, R.D. (2003). Nucleosomes unfold completely at a transcriptionally active promoter. *Mol. Cell* **11**, 1587–1598.
- Briggs, S.D., Bryk, M., Strahl, B.D., Cheung, W.L., Davie, J.K., Dent, S.Y., Winston, F., and Allis, C.D. (2001). Histone H3 lysine 4 methylation is mediated by Set1 and required for cell growth and rDNA silencing in *Saccharomyces cerevisiae*. *Genes Dev.* **15**, 3286–3295.
- Causton, H.C., Ren, B., Koh, S.S., Harbison, C.T., Kanin, E., Jennings, E.G., Lee, T.I., True, H.L., Lander, E.S., and Young, R.A. (2001). Remodeling of yeast genome expression in response to environmental changes. *Mol. Biol. Cell* **12**, 323–337.
- Clarke, A.S., Lowell, J.E., Jacobson, S.J., and Pillus, L. (1999). Esa1p is an essential histone acetyltransferase required for cell cycle progression. *Mol. Cell Biol.* **19**, 2515–2526.
- Cosma, M.P., Tanaka, T., and Nasmyth, K. (1999). Ordered recruitment of transcription and chromatin remodeling factors to a cell cycle- and developmentally regulated promoter. *Cell* **97**, 299–311.
- Deckert, J., and Struhl, K. (2001). Histone acetylation at promoters is differentially affected by specific activators and repressors. *Mol. Cell Biol.* **21**, 2726–2735.
- Ellenberger, T.E., Brandl, C.J., Struhl, K., and Harrison, S.C. (1992). The GCN4 basic region leucine zipper binds DNA as a dimer of uninterrupted alpha helices: crystal structure of the protein-DNA complex. *Cell* **71**, 1223–1237.
- Feng, Q., Wang, H., Ng, H.H., Erdjument-Bromage, H., Tempst, P., Struhl, K., and Zhang, Y. (2002). Methylation of H3-lysine 79 is mediated by a new family of HMTases without a SET domain. *Curr. Biol.* **12**, 1052–1058.
- Gregory, P.D., Schmid, A., Zavari, M., Munsterkotter, M., and Horz, W. (1999). Chromatin remodelling at the PHO8 promoter requires SWI-SNF and SAGA at a step subsequent to activator binding. *EMBO J.* **18**, 6407–6414.
- Harbison, C.T., Gordon, D.B., Lee, T.I., Rinaldi, N.J., Macisaac, K.D., Danford, T.W., Hannett, N.M., Tagne, J.B., Reynolds, D.B., Yoo, J., et al. (2004). Transcriptional regulatory code of a eukaryotic genome. *Nature* **431**, 99–104.
- Holstege, F.C., Jennings, E.G., Wyrick, J.J., Lee, T.I., Hengartner, C.J., Green, M.R., Golub, T.R., Lander, E.S., and Young, R.A. (1998). Dissecting the regulatory circuitry of a eukaryotic genome. *Cell* **95**, 717–728.
- Hope, I.A., and Struhl, K. (1985). GCN4 protein, synthesized in vitro, binds HIS3 regulatory sequences: implications for general control of amino acid biosynthetic genes in yeast. *Cell* **43**, 177–188.
- Humphrey, E.L., Shanji, A.F., Bernstein, B.E., and Schreiber, S.L. (2004). Rpd3p relocation mediates a transcriptional response to rapamycin in yeast. *Chem. Biol.* **11**, 295–299.
- Kireeva, M.L., Walter, W., Tchernajenko, V., Bondarenko, V., Kashlev, M., and Studitsky, V.M. (2002). Nucleosome remodeling induced by RNA polymerase II: loss of the H2A/H2B dimer during transcription. *Mol. Cell* **9**, 541–552.
- Kouzarides, T. (2002). Histone methylation in transcriptional control. *Curr. Opin. Genet. Dev.* **12**, 198–209.
- Krogan, N.J., Dover, J., Wood, A., Schneider, J., Heidt, J., Boateng, M.A., Dean, K., Ryan, O.W., Golshani, A., Johnston, M., et al. (2003a). The Paf1 complex is required for histone H3 methylation by COMPASS and Dot1p: linking transcriptional elongation to histone methylation. *Mol. Cell* **11**, 721–729.
- Krogan, N.J., Kim, M., Tong, A., Golshani, A., Cagney, G., Canadien, V., Richards, D.P., Beattie, B.K., Emili, A., Boone, C., et al. (2003b). Methylation of histone H3 by Set2 in *Saccharomyces cerevisiae* is linked to transcriptional elongation by RNA polymerase II. *Mol. Cell Biol.* **23**, 4207–4218.
- Kuo, M.H., Brownell, J.E., Sobel, R.E., Ranalli, T.A., Cook, R.G., Edmondson, D.G., Roth, S.Y., and Allis, C.D. (1996). Transcription-linked acetylation by Gcn5p of histones H3 and H4 at specific lysines. *Nature* **383**, 269–272.
- Kuo, M.H., Zhou, J., Jambeck, P., Churchill, M.E., and Allis, C.D. (1998). Histone acetyltransferase activity of yeast Gcn5p is required for the activation of target genes in vivo. *Genes Dev.* **12**, 627–639.
- Kurdistani, S.K., Robyr, D., Tavazoie, S., and Grunstein, M. (2002). Genome-wide binding map of the histone deacetylase Rpd3 in yeast. *Nat. Genet.* **31**, 248–254.
- Kurdistani, S.K., Tavazoie, S., and Grunstein, M. (2004). Mapping global histone acetylation patterns to gene expression. *Cell* **117**, 721–733.
- Larschan, E., and Winston, F. (2001). The *S. cerevisiae* SAGA complex functions in vivo as a coactivator for transcriptional activation by Gal4. *Genes Dev.* **15**, 1946–1956.
- Lee, C.K., Shibata, Y., Rao, B., Strahl, B.D., and Lieb, J.D. (2004). Evidence for nucleosome depletion at active regulatory regions genome-wide. *Nat. Genet.* **36**, 900–905.
- Lee, T.I., Rinaldi, N.J., Robert, F., Odom, D.T., Bar-Joseph, Z., Gerber, G.K., Hannett, N.M., Harbison, C.T., Thompson, C.M., Simon, I., et al. (2002). Transcriptional regulatory networks in *Saccharomyces cerevisiae*. *Science* **298**, 799–804.
- Lieb, J.D., Liu, X., Botstein, D., and Brown, P.O. (2001). Promoter-specific binding of Rap1 revealed by genome-wide maps of protein-DNA association. *Nat. Genet.* **28**, 327–334.
- Luger, K., Mader, A.W., Richmond, R.K., Sargent, D.F., and Richmond, T.J. (1997). Crystal structure of the nucleosome core particle at 2.8 Å resolution. *Nature* **389**, 251–260.
- Nagy, P.L., Cleary, M.L., Brown, P.O., and Lieb, J.D. (2003). Genomewide demarcation of RNA polymerase II transcription units revealed by physical fractionation of chromatin. *Proc. Natl. Acad. Sci. USA* **100**, 6364–6369.
- Narlikar, G.J., Fan, H.Y., and Kingston, R.E. (2002). Cooperation between complexes that regulate chromatin structure and transcription. *Cell* **108**, 475–487.
- Natarajan, K., Meyer, M.R., Jackson, B.M., Slade, D., Roberts, C., Hinnebusch, A.G., and Marton, M.J. (2001). Transcriptional profiling shows that Gcn4p is a master regulator of gene expression during amino acid starvation in yeast. *Mol. Cell Biol.* **21**, 4347–4368.
- Ng, H.H., Feng, Q., Wang, H., Erdjument-Bromage, H., Tempst, P., Zhang, Y., and Struhl, K. (2002a). Lysine methylation within the globular domain of histone H3 by Dot1 is important for telomeric silencing and Sir protein association. *Genes Dev.* **16**, 1518–1527.
- Ng, H.H., Robert, F., Young, R.A., and Struhl, K. (2002b). Genome-wide location and regulated recruitment of the RSC nucleosome-remodeling complex. *Genes Dev.* **16**, 806–819.
- Ng, H.H., Ciccone, D.N., Morshead, K.B., Oettinger, M.A., and Struhl, K. (2003a). Lysine-79 of histone H3 is hypomethylated at silenced loci in yeast and mammalian cells: a potential mechanism for position-effect variegation. *Proc. Natl. Acad. Sci. USA* **100**, 1820–1825.
- Ng, H.H., Robert, F., Young, R.A., and Struhl, K. (2003b). Targeted recruitment of Set1 histone methylase by elongating Pol II provides a localized mark and memory of recent transcriptional activity. *Mol. Cell* **11**, 709–719.
- O’Shea, E.K., Klemm, J.D., Kim, P.S., and Alber, T. (1991). X-ray structure of the GCN4 leucine zipper, a two-stranded, parallel coiled coil. *Science* **254**, 539–544.
- Oliphant, A.R., Brandl, C.J., and Struhl, K. (1989). Defining the sequence specificity of DNA-binding proteins by selecting binding sites from random-sequence oligonucleotides: analysis of yeast GCN4 protein. *Mol. Cell Biol.* **9**, 2944–2949.
- Peterson, C.L., and Laniel, M.A. (2004). Histones and histone modifications. *Curr. Biol.* **14**, R546–R551.
- Reid, J.L., Iyer, V.R., Brown, P.O., and Struhl, K. (2000). Coordinate regulation of yeast ribosomal protein genes is associated with targeted recruitment of Esa1 histone acetylase. *Mol. Cell* **6**, 1297–1307.
- Reinke, H., and Horz, W. (2003). Histones are first hyperacetylated and then lose contact with the activated PHO5 promoter. *Mol. Cell* **11**, 1599–1607.
- Reinke, H., Gregory, P.D., and Horz, W. (2001). A transient histone

hyperacetylation signal marks nucleosomes for remodeling at the PHO8 promoter in vivo. *Mol. Cell* 7, 529–538.

Ren, B., Robert, F., Wyrick, J.J., Aparicio, O., Jennings, E.G., Simon, I., Zeitlinger, J., Schreiber, J., Hannett, N., Kanin, E., et al. (2000). Genome-wide location and function of DNA binding proteins. *Science* 290, 2306–2309.

Robert, F., Pokholok, D.K., Hannett, N.M., Rinaldi, N.J., Chandy, M., Rolfe, A., Workman, J.L., Gifford, D.K., and Young, R.A. (2004). Global position and recruitment of HATs and HDACs in the yeast genome. *Mol. Cell* 16, 199–209.

Robyr, D., Suka, Y., Xenarios, I., Kurdistani, S.K., Wang, A., Suka, N., and Grunstein, M. (2002). Microarray deacetylation maps determine genome-wide functions for yeast histone deacetylases. *Cell* 109, 437–446.

Roh, T.Y., Ngau, W.C., Cui, K., Landsman, D., and Zhao, K. (2004). High-resolution genome-wide mapping of histone modifications. *Nat. Biotechnol.* 22, 1013–1016.

Santos-Rosa, H., Schneider, R., Bannister, A.J., Sherriff, J., Bernstein, B.E., Emre, N.C., Schreiber, S.L., Mellor, J., and Kouzarides, T. (2002). Active genes are tri-methylated at K4 of histone H3. *Nature* 419, 407–411.

Schubeler, D., MacAlpine, D.M., Scalzo, D., Wirbelauer, C., Kooperberg, C., van Leeuwen, F., Gottschling, D.E., O'Neill, L.P., Turner, B.M., Delrow, J., et al. (2004). The histone modification pattern of active genes revealed through genome-wide chromatin analysis of a higher eukaryote. *Genes Dev.* 18, 1263–1271.

Strahl, B.D., Grant, P.A., Briggs, S.D., Sun, Z.W., Bone, J.R., Caldwell, J.A., Mollah, S., Cook, R.G., Shabanowitz, J., Hunt, D.F., and Allis, C.D. (2002). Set2 is a nucleosomal histone H3-selective methyltransferase that mediates transcriptional repression. *Mol. Cell. Biol.* 22, 1298–1306.

Suka, N., Luo, K., and Grunstein, M. (2002). Sir2p and Sas2p oppositely regulate acetylation of yeast histone H4 lysine16 and spreading of heterochromatin. *Nat. Genet.* 32, 378–383.

Utey, R.T., Ikeda, K., Grant, P.A., Cote, J., Steger, D.J., Eberharter, A., John, S., and Workman, J.L. (1998). Transcriptional activators direct histone acetyltransferase complexes to nucleosomes. *Nature* 394, 498–502.

van Leeuwen, F., Gafken, P.R., and Gottschling, D.E. (2002). Dot1p modulates silencing in yeast by methylation of the nucleosome core. *Cell* 109, 745–756.

Vogelauer, M., Wu, J., Suka, N., and Grunstein, M. (2000). Global histone acetylation and deacetylation in yeast. *Nature* 408, 495–498.

Xiao, T., Hall, H., Kizer, K.O., Shibata, Y., Hall, M.C., Borchers, C.H., and Strahl, B.D. (2003). Phosphorylation of RNA polymerase II CTD regulates H3 methylation in yeast. *Genes Dev.* 17, 654–663.

Zhang, W., Bone, J.R., Edmondson, D.G., Turner, B.M., and Roth, S.Y. (1998). Essential and redundant functions of histone acetylation revealed by mutation of target lysines and loss of the Gcn5p acetyltransferase. *EMBO J.* 17, 3155–3167.

Accession Numbers

The microarray data described herein are available at ArrayExpress (<http://www.ebi.ac.uk/arrayexpress>) under the accession number E-WMIT-3.